

Relationship between the near-Earth interplanetary field and the coronal source flux: Dependence on timescale

M. Lockwood¹

Rutherford Appleton Laboratory, Chilton, Didcot, Oxfordshire, England, UK

Received 5 October 2001; revised 8 April 2002; accepted 19 April 2002; published 5 December 2002.

[1] The Ulysses spacecraft has shown that the radial component of the heliospheric magnetic field is approximately independent of latitude. This has allowed quantification of the total open solar flux from near-Earth observations of the interplanetary magnetic field. The open flux can also be estimated from photospheric magnetograms by mapping the fields up to the “coronal source surface” where the field is assumed to be radial and which is usually assumed to be at a heliocentric distance $r = 2.5R_S$ (a mean solar radius, $1R_S = 6.96 \times 10^8$ m). These two classes of open flux estimate will differ by the open flux that threads the heliospheric current sheet(s) inside Earth’s orbit at $2.5R_S < r < 1R_1$ (where the mean Earth-Sun distance, $1R_1 = 1 \text{ AU} = 1.5 \times 10^{11}$ m). We here use near-Earth measurements to estimate this flux and show that at sunspot minimum it causes only a very small ($\approx 0.5\%$) systematic difference between the two types of open flux estimate, with an uncertainty that is of order $\pm 24\%$ in hourly values, $\pm 16\%$ in monthly averages, and between -6% and $+2\%$ in annual values. These fractions may be somewhat larger for sunspot maximum because of flux emerging at higher heliographic latitudes. *INDEX TERMS:* 2164 Interplanetary Physics: Solar wind plasma; 2134 Interplanetary Physics: Interplanetary magnetic fields; 2199 Interplanetary Physics: General or miscellaneous; 2194 Interplanetary Physics: Instruments and techniques; *KEYWORDS:* open solar flux, heliospheric field

Citation: Lockwood M., Relationship between the near-Earth interplanetary field and the coronal source flux: Dependence on timescale, *J. Geophys. Res.*, 107(A12), 1425, doi:10.1029/2001JA009062, 2002.

1. Introduction

[2] The data taken by the Ulysses satellite, as it passed from the ecliptic plane to over the southern solar pole [Balogh *et al.*, 1995], showed that the radial component of the magnetic field in the heliosphere is approximately independent of latitude, once allowance has been made for the variation with heliocentric distance, r . A square law dependence on r is expected because flux tube area increases as r^2 and this is an important part of Parker spiral theory which explains observed heliospheric fields very well on annual timescales [Gazis, 1996; Stamper *et al.*, 1999]. Lockwood *et al.* [1999b] have also shown that the result of Balogh *et al.* also applied during for the pole-to-pole “fast” latitude scan during the perihelion pass and Smith *et al.* [2001] have shown it to be valid during the second ascent of Ulysses to the southern polar region. The first perihelion pass took place during the interval September 1994 to July 1995 when solar activity was low. Recent data from the second perihelion pass (December 2000 to October 2001) show that the result also holds at sunspot maximum (A. Balogh, private communication, 2002). This discovery reveals that the inner heliosphere is dominated by sheet, and not volume, currents and has been

explained by Suess and Smith [1996] and Suess *et al.* [1996] in terms of the pressure transverse to the flow in the expanding solar wind at r between about $1.5R_S$ and $10R_S$ where the plasma beta is low (the mean solar radius, $R_S = 6.96 \times 10^8$ m): nonradial flow allows the field to redistribute during its early expansion to give constant tangential magnetic pressure and thus constant radial field.

[3] Because of this result, the radial field seen at Earth B_{rE} can be used to compute the total flux threading a heliocentric sphere of radius $R_1 = 1 \text{ AU} = 1.5 \times 10^{11}$ m. From this, the (signed) open flux estimate is

$$F'_s = 4\pi R_1^2 |B_{rE}| / 2. \quad (1)$$

The factor 2 arises because half the flux through this surface is outward (away from the Sun) and half is inward. By neglecting the flux F_{cs} threading the heliospheric current sheet(s) at r between $2.5R_S$ and R_1 (see Figure 1) several authors have equated this to the coronal source flux F_s , the total flux leaving the solar corona and entering the heliosphere by threading a hypothetical surface where the field is purely radial this is called “the coronal source surface” and is usually taken to be approximately spherical and at $r = 2.5R_S$ [e.g., Wang and Sheeley, 1995].

[4] Some additional support for the use of equation (1) comes from coronal source flux estimates from measurements of the line-of-sight component of the photospheric field (at $r = 1R_S$). In deriving this line-of-sight component of the field from magnetograph data, a latitude-dependent

¹Also at Department of Physics and Astronomy, University of Southampton, Southampton, Hampshire, UK.

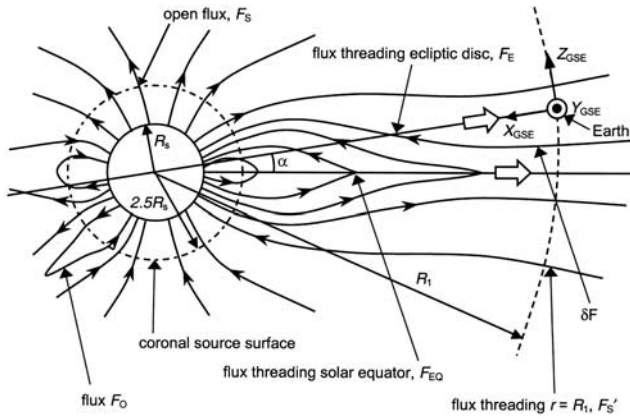


Figure 1. Idealized schematic of open solar flux near solar minimum. The total flux threading of the coronal source surface (dot-dashed line, at $r \approx 2.5R_s$) is F_s and contains the flux $F'_s = (2\pi R_1)|B_{rE}|$ that threads a heliocentric sphere of radius $R_1 = 1$ AU, plus the flux F_{EQ} that threads the solar equator inside the Earth's orbit and the open flux F_O that cuts neither the 1 AU sphere nor the ecliptic plane. The flux F_E threading the ecliptic plane at $r < R_1$ differs from F_{EQ} by the flux δF . Field lines contributing to the fluxes F_s , F'_s , F_{EQ} , F_O , F_E , and δF are all labelled.

“line saturation” correction factor must be applied [Wang and Sheeley, 1995, 2002]. The photospheric field is assumed to be radial so that it can be determined from its line-of-sight component (so there is no information from over the solar poles). The open flux is then estimated using a method such as the potential field source surface (PFSS) procedure [Schatten *et al.*, 1969], in which the corona is assumed to be current-free between the photospheric surface and the coronal source surface. The method is applied to full Carrington rotation periods and assumes that all fields are constant over these intervals. Despite these several assumptions and approximations, Wang and Sheeley [1995, 2002] were able to match to the radial field seen at Earth during solar cycles 20–23, again using the assumption that B_r is independent of latitude in the heliosphere, as found from the Ulysses observations.

[5] The PFSS procedures, therefore, compute the flux F_s threading the hypothetical source surface, usually assumed to be at $r = 2.5R_s$. The near-Earth methods, on the other hand, compute the flux threading the spherical surface at $r = 1R_1$, F'_s . In this paper, we investigate the flux F_{cs} , which, at any one time, threads the coronal source surface but closes by crossing the heliospheric current sheet (or sheets) inside the sphere $r = 1R_1$. This flux is a systematic difference between the PFSS and near-Earth estimates. Figure 1 is an idealized schematic of the heliospheric field near sunspot minimum, showing the coronal source surface and the sphere at $r = R_1$.

[6] From Figure 1 the difference between the two estimates of open flux is the flux threading the current sheet(s) F_{cs} at ($2.5R_s < r < R_1$):

$$F_s = F'_s + F_{cs} = \{2\pi R_1^2 |B_{rE}|\} + F_{EQ} + F_O, \quad (2)$$

Where F_{EQ} is the open flux that threads the solar equator at $2.5R_s < r < R_1$ and F_O is the open flux that threads neither the solar equator nor the sphere at $r = R_1$. In this paper, we use

interplanetary measurements of the magnetic field and the solar wind flow to quantify the flux threading the ecliptic plane F_E , which differs from F_{EQ} by a difference δF (which is shown to be relatively small). Field lines contributing to the fluxes F_E , F_O , F_{EQ} , and δF are all shown in Figure 1. The difference between the two estimates (F'_s from equation (1) and F_s from equation (2)) is studied as a function of averaging timescale for the simpler case of solar minimum conditions.

2. Data Analysis

[7] We employ hourly averages of interplanetary magnetic field and solar wind velocity components, as observed by a variety of near-Earth satellites. These data are a continuation of the “Omnitape” data set [Couzens and King, 1986]. We use data from the start of January 1979 to the end of September 1999, an interval that covered almost all of 2 solar cycles and that also gave good coverage in terms of the fraction of the total time for which both solar wind speed and interplanetary magnetic field observations were available, particularly before 1983 and after 1994. Out of a possible 181,457 hours, usable data were available for 100,160 (55%). The data are supplied in the Geocentric Solar Ecliptic (GSE) frame of reference and this is ideal for the calculations made here.

2.1. Autocorrelation Functions of Interplanetary Parameters

[8] For the analysis presented here, data gaps are a particular problem. To minimize their effect we have linearly interpolated over gaps that are sufficiently short. To estimate how long an interval a given parameter can be interpolated over, we looked at its autocorrelation function (acf). Figure 2 shows the acfs for hourly means of the radial component of the solar wind speed $V_r = -[V_x]_{GSE}$, the northward component of the IMF $[B_z]_{GSE}$, and the coronal

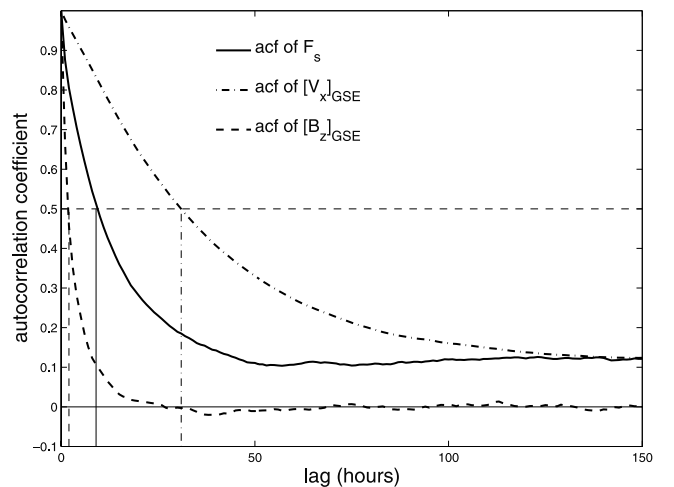


Figure 2. Autocorrelation functions (acf, autocorrelation coefficient as a function of lag) of hourly means of the coronal source flux F'_s estimated from equation (1) (solid line); the radial solar wind velocity, $V_r = -[V_x]_{GSE}$ (dot-dashed line); and the northward component of the interplanetary magnetic field $[B_z]_{GSE}$ (dashed line). The corresponding vertical lines mark the lag where the acf falls to 0.5 (at 9, 31, and 2 hours, respectively).

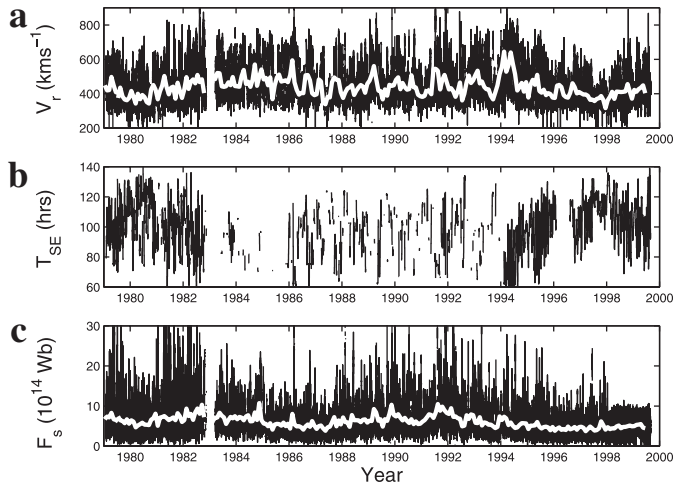


Figure 3. Variations of (a) the radial solar wind flow speed V_r ; (b) the solar wind transit time from the coronal source surface to earth, T_{SE} ; and (c) the coronal source flux F_s' estimated from equation (1). The black lines are hourly values, and the superposed white lines are monthly means.

source flux F_s' , computed from near-Earth measurements using equation (1). In each case, the corresponding vertical dashed line marks the lag at which the acf falls to 0.5. It can be seen that this occurs at 31, 2, and 9 hours for $[V_x]_{GSE}$, $[B_z]_{GSE}$, and F_s' , respectively. These lags are a measure of the “persistence” or “conservation” in these data sequences, i.e., the tendency for values to remain the same. We here adopt the criterion that we can linearly interpolate over data gaps of length 30, 1, and 8 hours in these respective cases. The analysis was repeated using no interpolation and no substantial differences resulted in any plot presented, other than an increase in the statistical noise in some cases because of the reduced number of available samples.

2.2. Interplanetary Sun-to-Earth Transit Times

[9] In order to compute the total flux threading the ecliptic plane sunward of 1 AU, F_E , we need to know the time T_{SE} for all that flux to be carried past the Earth’s orbit. This is the time for the flux that has just emerged through the coronal source surface at $r = 2.5R_s$ to reach the observation point near $r = R_1$. If the solar wind were constant in time and space, with its mode value at Earth of $V_r = 370 \text{ km s}^{-1}$, T_{SE} would be 112.6 hours. However, V_r fluctuates considerably (hourly values range between 250 and 950 km s^{-1} [Hapgood et al., 1991]). Figure 2 shows that on the timescale of $T_{SE} = 112.6$ hours discussed above, there is only a small coherence in the solar wind flow speed, whereas there is considerable coherence (acf ≈ 0.5) on lag timescales of order ± 30 hours (corresponding to a radial spatial scale of order ± 0.25 AU for $V_r = 370 \text{ km s}^{-1}$). Thus we need to allow for variability of the solar wind flow speed during the transit time, but also still allow for the fact that the solar wind speed data series has conservation, revealing that the flow at any one location influences the speed of flow at least 0.25 AU ahead and 0.25 AU behind that location, on average. The Sun-to-Earth transit time T_{SE} for a solar wind element observed at time t_0 is given by the integral

$$\int_{t_0 - T_{SE}}^{t_0} V_r(r, t) dt = \{R_1 - 2.5R_s\} \quad (3)$$

where $V_r(r, t)$ is the radial speed of the solar wind element at radial distance r and time t . The problem is that we do not know $V_r(r, t)$, rather we have observations of $V_r(R_1, t)$. We here make an allowance for the variability in V_r by making two different, simple assumptions to enable us to use equation (3). Method 1 assumes that $V_r(r, t)$ is equal to the $V_r(R_1, t)$ at the same time, t . This assumption would be valid if the correlation length of the solar wind flow speed was > 1 AU, instead of ~ 0.5 AU, as discussed above. Method 2 assumes that each parcel of solar wind maintains the same velocity at all r to R_1 and thus $V_r(r, t)$ is equal to $V_r(R_1, t + T_{rE})$ where T_{rE} is the transit time from r to R_1 : in this case, the correlation length would be less than the distance travelled by the solar wind during the sampling interval of one hour (~ 0.01 AU). Using methods 1 and 2, the integral (3) yields T_{ES1} and T_{ES2} , respectively. In general, the two procedures yield similar results but T_{ES1} is systematically slightly higher than T_{ES2} . This is demonstrated by the distribution of values of $\{2(T_{ES1} - T_{ES2}) / (T_{ES1} + T_{ES2})\}$ which has a mean of +2.4%, a median of +4.7%, a mode of 7%, with lower and upper deciles (i.e., the values exceeded 90% and 10% of the time) of -17% and $+18\%$. Thus T_{ES1} and T_{ES2} agree to within about 20%. We here use the average $T_{ES} = (T_{ES1} + T_{ES2})/2$, consistent with the coherence length of ~ 0.5 AU. We find that T_{ES} , T_{ES1} and T_{ES2} give almost identical distributions for F_E , discussed in the next section, and thus the results do not depend greatly on the method used to compute T_{ES} .

[10] This computation of T_{ES} requires continuous V_r data. The number of valid hourly $V_x(R_1, t)$ values in the 1988–1999 data set is 88,376, and with linear interpolation over data gaps of up to 30 hours duration, this rises to 90,902. The number of T_{ES} values obtained from continuous $V_x(R_1, t)$ data series (with interpolation over data gaps shorter than 30 hours) is 53,886.

[11] Figure 3 shows the time variations between 1979 and 1999 of hourly values of (a) the radial flow speed V_r , (b) the transit time T_{SE} , and (c) the open flux estimate F_s' , deduced from equation (1). The white lines superposed show the monthly averages. The solar cycle can be seen in the source

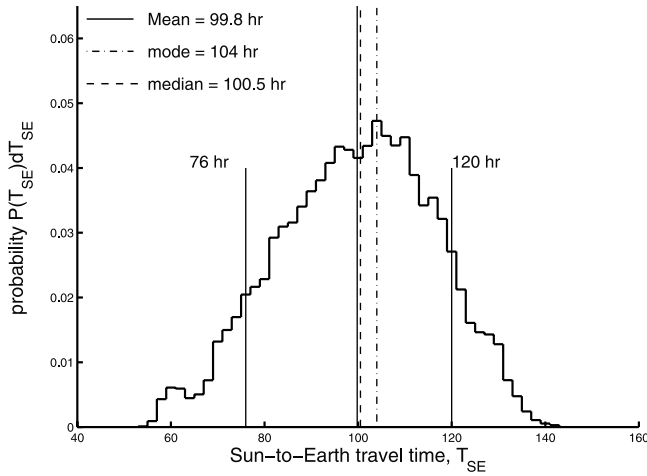


Figure 4. The distribution of solar wind transit times from $r = 2.5R_s$ to $r = R_1 = 1$ AU, T_{SE} . The full length solid vertical line gives the mean (99.8 hours), and the half-length vertical solid lines give the lower and upper decile values (76 and 120 hours). The dot-dashed and dashed lines give the mode (104 hours) and median (100.5 hours), respectively.

flux with higher monthly averages just after solar maximum when there are more short-lived spikes in hourly values. In the declining phase of the solar cycle (particularly in 1994) the flow speed is somewhat enhanced, as expected because the Earth intersects fast solar wind streams emanating from the low-latitude extensions of coronal holes. This is reflected in lower values of the transit time, T_{SE} .

[12] The distribution of derived T_{SE} values is given in Figure 4. The range of values is 53–139 hours. The mean and median values are both near 100 hours, and the mode value at 104 hours is also somewhat lower than that derived from the mode of the solar wind speed distribution. The upper and lower deciles are 76 and 120 hours, respectively.

2.3. Flux Threading the Ecliptic Plane at $2.5R_s < r < R_1$

[13] The hourly averages of $[V_x]_{GSE}$ and $[B_z]_{GSE}$ can give hourly values of the electric field in the Y direction (antiparallel to Earth's orbital motion, see Figure 1) from $\underline{E} = -\underline{V} \times \underline{B}$. By Faraday's law, this is the flux transport rate per unit length of the Earth's orbit. Averaging over longitudinal structure, the total flux transport rate across $r = R_1$ would be:

$$dF/dt = (2\pi R_1)[V_x]_{GSE}[B_z]_{GSE} \quad (4)$$

and the total flux transported over R_1 in the transit time T_{SE} is the flux threading the ecliptic at $2.5R_s < r < R_1$, F_E , which at time t gives

$$F_E = \int_{t_{SE}^-}^{t_0} (2\pi R_1)[V_x]_{GSE}[B_z]_{GSE} dt \quad (5)$$

For the 53,886 values for which T_{SE} can be computed, there are 29,544 for which there are also full sets of $[B_z]_{GSE}$ values over the interval T_{SE} (with only 1 hour data gaps, which can be filled by linear interpolation).

[14] Figure 5 shows as a dashed line the distribution of the hourly F_E values derived from equation (5), along with

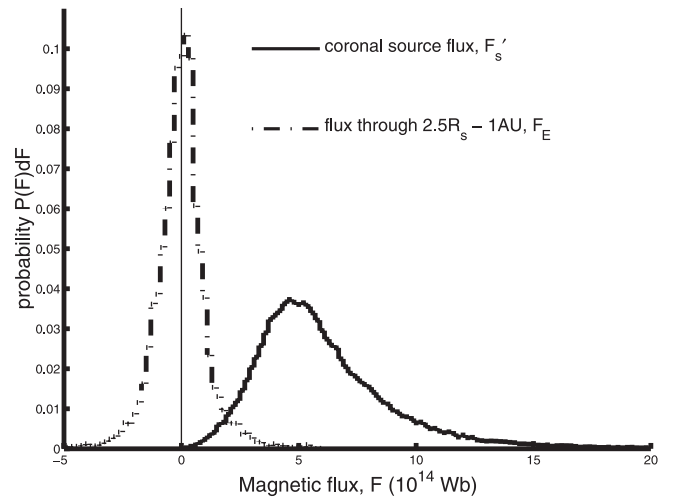


Figure 5. Distributions of hourly estimates of (solid line) coronal source flux, F'_s , and of (dashed line) the flux F_E threading the ecliptic disc between $r = 2.5R_s$ and $r = R_1 = 1$ AU.

the F'_s values computed from equation (1). It can be seen that F_E is generally considerably smaller than F'_s and is distributed around mode, mean and median values that are all near zero. The mean value of (F_E/F'_s) is -0.005 . Thus F_E does not introduce any significant systematic error into F'_s (<0.5%) but does add an uncertainty to the individual hourly values. Figure 6 shows the distribution of F_E as a ratio of the F'_s values. Of the 29,544 F_E values, a simultaneous F'_s value is available for 27,792. The mean and median values of the (F_E/F'_s) distribution are both close to zero (-0.006 and 0.001) with a slightly larger mode (0.060) and upper and lower deciles of 0.22 and -0.26 . From Figure 6 we can say that 90% of F_E values are less than about 24% of the simultaneous F'_s values in hourly averages.

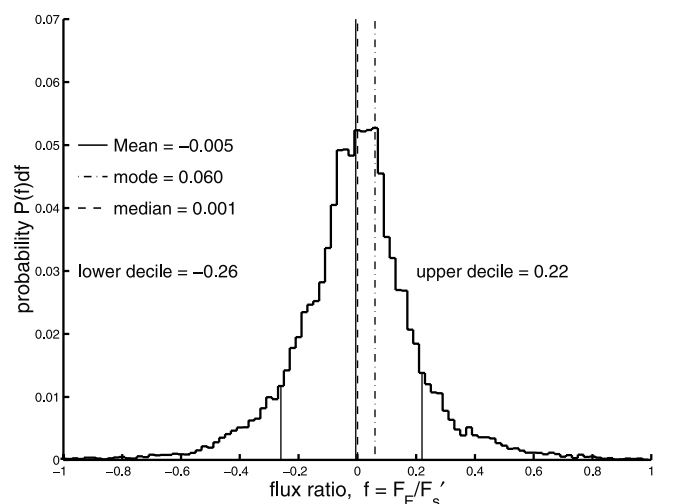


Figure 6. The distribution of hourly values of the ratio of fluxes $f = F_E/F'_s$. The full length solid vertical line gives the mean (-0.005), and the half-length vertical solid lines give the lower and upper decile values (-0.26 and 0.22). The dot-dashed and dashed lines give the mode (0.060) and median (0.001), respectively.

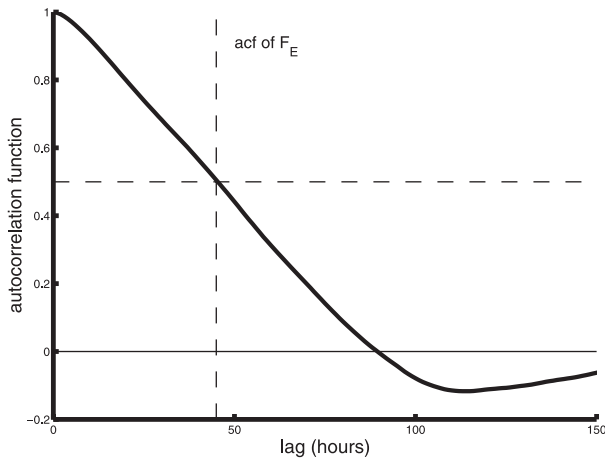


Figure 7. Autocorrelation function (acf, autocorrelation coefficient as a function of lag) of hourly values of the flux threading the ecliptic plane inside Earth's orbit, F_E . The dashed lines mark the lag where the acf falls to 0.5 (45 hours).

Thus we can say that neglecting F_E and applying equation (1) to hourly values gives an estimate of F'_s that is accurate to about 24%. Figure 7 shows the acf of the F_E values. It can be seen that the autocorrelation coefficient falls to 0.5 with a lag of about 3.5 days and is negative thereafter. Thus averaging over periods of a solar rotation or greater will tend to reduce the F_E values because positive and negative hourly F_E values tend to cancel out.

2.4. Monthly and Annual Averages

[15] The hourly averages presented in Figure 6 yield 152 monthly means if we require that more than 75% of the hours in the month have data. These yield 47 full 12 month running means of monthly data.

[16] Figure 8 shows the distribution of monthly (dashed line) and annual (solid line) F_E/F'_s values. For the monthly values the upper and lower decile values of this ratio are 0.16 and -0.17 , which is a smaller spread than for the hourly values. For the annual means, the deciles fall yet further in magnitude to -0.06 and 0.02 .

[17] The perihelion passes of Ulysses show that the assumption that the radial heliospheric field B_r is independent of latitude introduces errors of about 5% into the open flux, as estimated by equation (1) (M. Lockwood et al., The accuracy of open solar flux estimates from near-Earth measurements of the interplanetary magnetic field: Analysis of the first two perihelion passes of the Ulysses spacecraft, submitted to *Annales Geophysicae*, 2002, hereinafter referred to as Lockwood et al., submitted reference, 2002). Combining with the (independent) errors due to F_E deduced here, this yields a total error of 17% in F'_s values for the monthly data, the biggest contribution to which is the flux F_E . For the annual data the error is 6%, with the largest uncertainty caused latitudinal gradients in B_r and the use of equation (1).

3. Discussion and Conclusions

[18] In order to understand the implications of these F_E/F'_s values, it is useful to consider the various contributions to F_E . These include the tilting of the heliospheric field toward and away from the ecliptic by the warped heliospheric

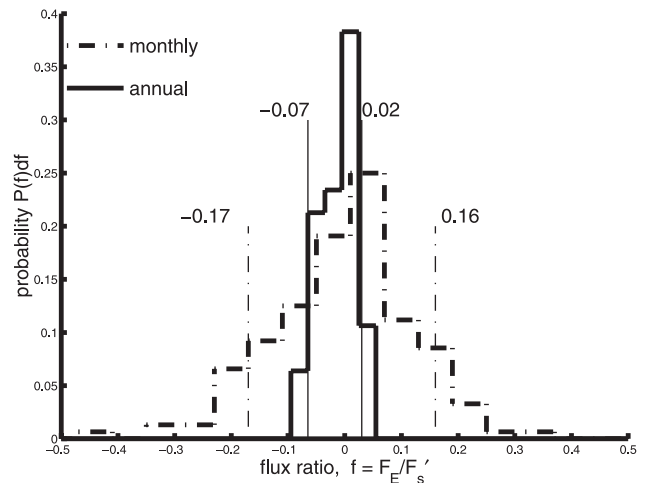


Figure 8. The distribution of monthly values (dot-dashed line) and annual values (solid line) of the ratio of fluxes $f = F_E/F'_s$. The vertical dot-dashed lines give the lower and upper decile values for monthly data (-0.17 and 0.16), and the vertical solid lines give the corresponding values for the annual data (-0.07 and 0.02).

current sheet, as well as by transient events such as corotating interaction regions and coronal mass ejections. Averaging over sufficiently long intervals would mean that these contributions would cancel each other to zero. The remaining contributions are newly emerged open flux and any disconnected flux. Averaging would give the net newly emerged, connected flux that has yet to reach $r = R_1$ (i.e., the difference between F'_s and F_s).

[19] The flux threading the ecliptic disc sunward of the Earth, F_E , gives a difference between the F_s and F'_s estimates that is of order $\pm 20\%$ in hourly values, $\pm 16\%$ in monthly averages and just 2% in annual values. These differences should be compared with the uncertainties introduced into F'_s by assuming that the radial field is independent of latitude which are of order 5% (Lockwood et al., submitted manuscript, 2002).

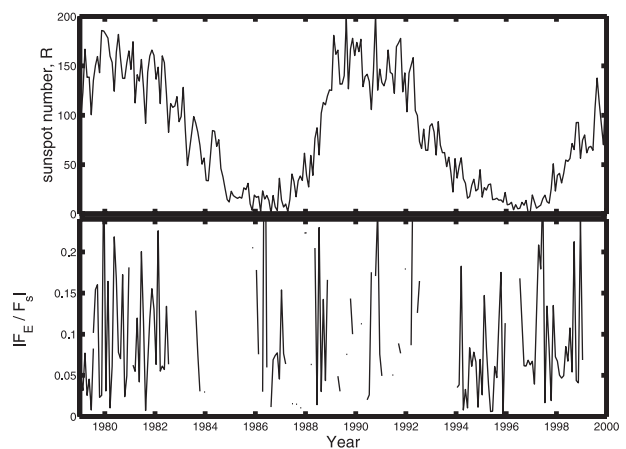


Figure 9. Variations of (top) sunspot number R and (bottom) the flux threading the ecliptic plane inside Earth's orbit, F_E , as a ratio of the open flux estimate F'_s .

[20] Thus far we have not considered the flux F_O nor the flux δF which threads the ecliptic disc but not the solar equator (see Figure 1). The flux δF arises because the solar equator is tilted with respect to the ecliptic plane and depends on the heliographic latitude λ_E of the Earth, which varies over the range of roughly $\pm 6^\circ$ for monthly mean data. Given that the radial field component is independent of λ_E , we have from the surface area of the segment of the sphere at $r = R_1$ that is subtended by the ecliptic and solar equatorial planes:

$$|\delta F| = |B_{rE}|(4\lambda_E R_1^2) = (\lambda_E/\pi)F'_s, \quad (6)$$

where F'_s is given by equation (1). Thus F_E is a good estimate of the flux threading the solar equatorial plane to within an error of $\pm(6/180)F'_s$, i.e., to within 3.3% of the monthly F'_s estimates. Because λ_E is known as a function of time-of-year, this error could be corrected for using equation (6) and anyway averages to zero in annual means.

[21] Equation (2) shows that flux F_O is also an uncertainty in the coronal source flux estimate. At sunspot minimum, the heliospheric field has a roughly dipolar configuration with clear northern and southern poles and thus open flux that remains within the heliocentric sphere of radius R_1 , and yet does not thread the solar equator, can be neglected (i.e., $F_O \approx 0$). However, this may well not be true at sunspot maximum and the open flux estimate based on near-Earth observations, F'_s , may underestimate the true source flux by a significant flux F_O as well as the flux F_E estimated here. Figure 9 compares the variation of F_E/F'_s estimates with the solar cycle and no consistent variation can be deduced and thus the total systematic uncertainty $(F_E + F_O)/F'_s$ is likely to be somewhat larger at sunspot maximum than at sunspot minimum. It is possible that the flux F_O , like F_E , averages to near zero in annual means, even at sunspot maximum because there are indications that, even at solar maximum, there is only a single current sheet [Smith *et al.*, 2001] and the Earth would spend equal amounts of time on the two sides of that sheet.

[22] We conclude that the difference between near-Earth and coronal source surface estimates of the total open solar flux from near-Earth measurements, caused by the flux threading the current sheet sunward of the Earth, gives a very small systematic error ($\approx 0.5\%$) at sunspot minimum, and within a small uncertainty of $\pm 2\%$ in annual data. At

sunspot maximum these uncertainties may be increased by open flux that does not reach $r = R_1$ but which also does not cut the solar equator.

[23] **Acknowledgments.** The author is grateful to the World Data Center system for collecting, archiving, and distributing the interplanetary data and to the many scientists who contributed these data to the WDC network. He also thanks A. Balogh and R. Forsyth for valuable discussions. This work was supported by the U.K. Particle Physics and Astronomy Research Council.

[24] Shadia Rafai Habbal thanks Robert Forsyth and another referee for their assistance in evaluating this paper.

References

- Balogh, A., E. J. Smith, B. T. Tsurutani, D. J. Southwood, R. J. Forsyth, and T. S. Horbury, The heliospheric field over the south polar region of the Sun, *Science*, 268, 1007–1010, 1995.
- Couzens, D. A., and J. H. King, *Interplanetary Medium Data Book-Supplement 3*, Natl. Space Sci. Data Cent., Goddard Space Flight Cent., Greenbelt, Md., 1986.
- Gazis, P. R., Solar cycle variation of the heliosphere, *Rev. Geophys.*, 34, 379–402, 1996.
- Hapgood, M. A., G. Bowe, M. Lockwood, D. M. Willis, and Y. Tulunay, Variability of the interplanetary magnetic field at 1 A. U. over 24 years: 1963–1986, *Planet. Space Sci.*, 39, 411–423, 1991.
- Lockwood, M., R. Stamper, and M. N. Wild, A doubling of the Sun's coronal magnetic field during the last 100 years, *Nature*, 399, 437–439, 1999a.
- Lockwood, M., R. Stamper, M. N. Wild, A. Balogh, and G. Jones, Our changing Sun, *Astron. Geophys.*, 40, 4.10–4.16, 1999b.
- Schatten, K. H., J. M. Wilcox, and N. F. Ness, A model of interplanetary and coronal magnetic fields, *Sol. Phys.*, 6, 442–455, 1969.
- Smith, E. J., A. Balogh, R. J. Forsyth, and D. J. McComas, Ulysses in the south polar cap at solar maximum: Heliospheric magnetic, *Geophys. Res. Lett.*, 28, 4159–4162, 2001.
- Stamper, R., M. Lockwood, M. N. Wild, and T. D. G. Clark, Solar causes of the long-term increase in geomagnetic activity, *J. Geophys. Res.*, 104, 28,325–28,342, 1999.
- Suess, S. T., and E. J. Smith, Latitudinal dependence of the radial IMF component—Coronal imprint, *Geophys. Res. Lett.*, 23, 3267–3270, 1996.
- Suess, S. T., E. J. Smith, J. Phillips, B. E. Goldstein, and S. Nerney, Latitudinal dependence of the radial IMF component—Interplanetary imprint, *Astron. Astrophys.*, 316, 304–312, 1996.
- Wang, Y.-M., and N. R. Sheeley Jr., Solar implications of Ulysses interplanetary field measurements, *Astrophys. J.*, 447, L143–L146, 1995.
- Wang, Y.-M., and N. R. Sheeley Jr., Sunspot activity and the long-term variation of the Sun's open magnetic flux, *J. Geophys. Res.*, doi:10.1029/2001JA000500, in press, 2002.

M. Lockwood, World Data Centre C-1 for Solar-Terrestrial Physics, Space Science Department, Rutherford Appleton Laboratory, Chilton, Didcot, Oxfordshire OX11 0QX, UK. (m.lockwood@rl.ac.uk)